



Article

Investigation of Thermal Bridges of a New High-Performance Window Installation Using 2-D and 3-D Methodology

Jolanta Šadauskienė^{1,*}, Juozas Ramanauskas^{1,2}, Dorota Anna Krawczyk³ , Eglė Klumbytė^{1,*} and Paris A. Fokaides^{1,4} 

¹ Faculty of Civil Engineering and Architecture, Kaunas University of Technology, Studentų Str. 48, LT-51367 Kaunas, Lithuania; juozas.ramanauskas@ktu.lt (J.R.); eng.fp@frederick.ac.cy (P.A.F.)

² Building Physics Laboratory of Institute of Architecture and Construction, Kaunas University of Technology, Tunelio Str. 60, LT-44405 Kaunas, Lithuania

³ Faculty of Civil Engineering and Environmental Sciences, Bialystok University of Technology, Wiejska 45 E, 15-351 Bialystok, Poland; d.krawczyk@pb.edu.pl

⁴ School of Engineering, Frederick University, Frederickou Str., Nicosia 1036, Cyprus

* Correspondence: jolanta.sadauskiene@ktu.lt (J.S.); egle.klumbyte@ktu.lt (E.K.)

Abstract: The investigation of building elements regarding energy saving is a paramount issue, with EU Directives driving achievement goals, focusing on buildings' energy performance and energy efficiency. This work focuses on investigating thermal bridges in a new high-performance window installation. This work aims to investigate the thermal properties of windows installed in the thermal insulation layer and to compare different installation methods and thermal bridge evaluation methodologies from the point of view of thermal physics. The results show that comparing the obtained values of the thermal bridge according to two- and three-dimensional domain (2-D and 3-D) calculation methods, the values show a difference of 68%. After examining the method of installing a new high-performance window in the thermal insulation layer, the effect of installing a window on the wall of a building is highlighted in this work. Given that windows are the most thermally conductive elements in a building, this paper provides guidance for both the scientific community and practitioners regarding trends in thermal bridges that change completely when using different assessment methods.

Keywords: thermal bridges; thermal transmittance; thermal insulation; passive energy buildings; window; building envelop



Citation: Šadauskienė, J.; Ramanauskas, J.; Krawczyk, D.A.; Klumbytė, E.; Fokaides, P.A. Investigation of Thermal Bridges of a New High-Performance Window Installation Using 2-D and 3-D Methodology. *Buildings* **2022**, *12*, 572. <https://doi.org/10.3390/buildings12050572>

Academic Editors: Yaolin Lin and Wei Yang

Received: 23 March 2022

Accepted: 26 April 2022

Published: 29 April 2022

Publisher's Note: MDPI stays neutral with regard to jurisdictional claims in published maps and institutional affiliations.



Copyright: © 2022 by the authors. Licensee MDPI, Basel, Switzerland. This article is an open access article distributed under the terms and conditions of the Creative Commons Attribution (CC BY) license (<https://creativecommons.org/licenses/by/4.0/>).

1. Introduction

The universal climate change problem has made it crucial for the European Union to invest in energy-saving methods. For this reason, members of the European Union have created an integrated national energy and climate plan from 2021 to 2030 [1]. The Energy Union and the Energy and Climate Policy Framework for 2030 pledge to reduce the amount of emitted gas, which is known to cause the greenhouse effect, by at least 40% compared to the amount emitted in 1990. According to the data of 2014, buildings used approximately 40% of all the energy generated in the EU countries. They emitted more than a third of the universally emitted amount of CO₂ gas [2]. Hence, it was concluded that the buildings sector has much potential to save energy.

Legal requirements for the new generation of buildings are stated in the renewed Directive (EU) 2018/844 [3], which focuses on the energy performance of buildings and energy efficiency. The Union's goal to develop an effective energy system by 2050 is difficult, since breakthroughs in energy efficiency move slowly. In 2014, about 3% of European buildings were Nearly Zero Energy Buildings (NZEB). That means 97% of the buildings were of low energy efficiency [4]. Currently, about 75% of buildings in the European Union are not energy efficient, but in 2050, 85–95% of them will still be in use.

Much effort is being put into renewing and supplementing the buildings' funds, because countless buildings were previously built following low energy usage efficiency standards. Nevertheless, only 1% of buildings are being efficiently renovated each year. For this reason, decisive action is required in order to achieve Europe's climate-neutral (net zero emissions) goals by 2050. According to the European Commission's 17 September Communication, due to Europe's 2030 climate ambitions [5], this norm must increase twice in order to achieve a more ambitious 2030 climate target of at least 55%. The Commission determined that renovation would be needed at an average rate of 3% annually in order to cost-effectively implement the Union's energy efficiency ambitions. For this reason, on 14 October 2020, the Commission presented a new renovation strategy called "A Renovation Wave for Europe—Greening our buildings, creating jobs, improving lives" [6].

In most European cities, buildings appeared during the past few decades and have not been properly taken care of for a long time. In most cases, buildings cannot satisfy modern requirements related to the quality of accommodation, energy usage efficiency, economy, and environmental protection. Doubtlessly, to achieve sustainability, one must emphasize the modern integrated renovation of already-built buildings and take notice of the usage of renewable energy and building insulation, heating, ventilation, and air conditioning (HVAC).

1.1. Thermal Bridge

One of the ways to effectively renovate buildings is to apply new high-performance windows. However, judging from experience, the low energy efficiency is often related to low quality of construction. Correct window installation is still one of the most difficult hurdles that must be overcome to achieve a higher energy efficiency in buildings [7]. Thermal imaging performed by professionals clearly shows thermal bridges at window openings (Figure 1) [8].

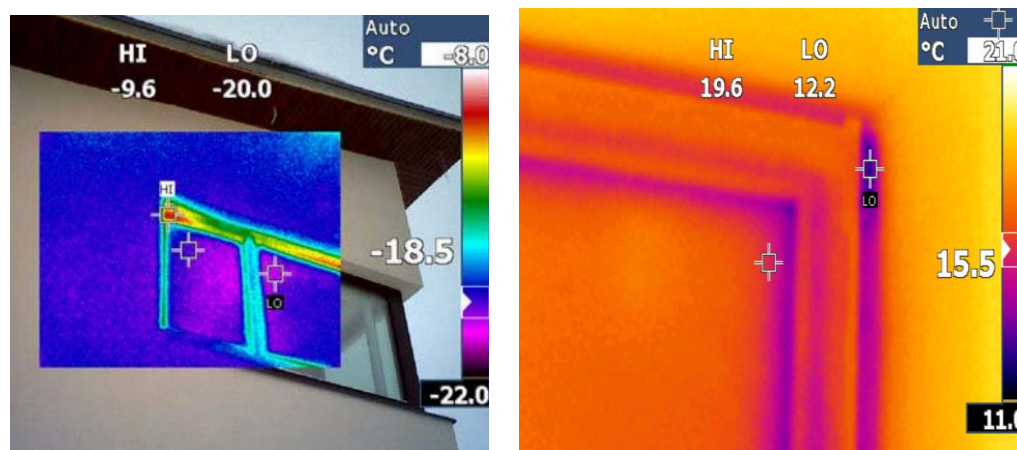


Figure 1. Thermal images of thermal bridges at window openings.

Thermal bridges are caused by full or partial penetration of the building envelope by materials with different thermal conductivities, changes in fabric thickness, and/or differences between internal and external areas, such as those found at wall/floor/ceiling junctions) [9]. According to a literature review, the total impact of thermal bridges on heating energy demand is generally significant, ranging from 5% to 39% [10–13]. The factors mentioned above are determined by weather conditions, insulation level, thermal bridge constructive solution, building type (use and geometry), and the method used to implement its effect within the calculation of the building energy demand [14].

Thermal bridges can impact a single point, a linear area, or an entire spatial configuration. Typically, the linear thermal bridges (LTB) that occur at the junction of two or more building envelope elements are evaluated in the calculations of the building's

energy demand. Several scientific studies have been conducted in which LTB was investigated using various calculation and simulation methodologies, such as static/dynamic and 1D/2D/3D [15–18].

The majority of studies present empirical LTB dependences, which determine the linear thermal transmittance value of a specific construction element [19]. On these foundations, numerical calculation software and catalogues have been developed. The European Standard EN ISO 14683 contains seventy-six cases referring to eight thermal bridge typologies (roofs, corners, intermediate floors, internal walls, slab-on-ground floors, suspended ground floors, pillars, window and door openings), and is one of the most widely used atlases. On the other hand, these atlases provide thermal bridge values calculated using the 2-D method. These calculations exclude point thermal bridges (PTB), which are formed by thermally conductive fasteners such as waxes, varnishes, etc. In terms of PTB, the effect of PTB is often neglected in analyses aimed at defining a building's energy performance. This study also addresses the significance of PTB in the calculation of thermal losses from thermal bridges in window installations.

1.2. A New High-Performance Window Installation

To partly resolve this problem, a new requirement was included in the Lithuanian national document [20], which stated that the thermal transmittance of a linear thermal bridge (LTB) of an NZEB or passive house must be a maximum of $0.05 \text{ W}/(\text{m}\cdot\text{K})$. However, attaining this value presents a severe difficulty for project designers and builders [21]. However, a new method of installing window frames directly onto thermal insulation layers has been found to reduce the effect of LTB [22].

Nowadays, a few alternative installation solutions are applied in the practical area of construction. Most window frameworks are pendent on reinforced anchor brackets (Figure 2a) or on rectangular wooden frames (chipboard) (Figure 2b) that are installed on a wall. However, these different cases of window mounting do not ensure that thermal bridges at the junction of wall and window will be avoided. Insufficiently isolated joints of window frames and facade walls increase the impact of building thermal leaks, and it does not ensure the required value of the airtightness of passive house, which must be equal to 0.6 air change rate at 50 Pa per hour. Furthermore, it is important to mention that the possibility of condensation and humidity increases when using the mentioned window mounting methods [23,24]. In this way, the building may lose its passive house status because of window installation defects [25,26].



Figure 2. System of window installation in the insulation layer: (a) on anchor brackets [27]; (b) on chipboard frame [28].

It is often incorrectly thought that by installing a window in the isolation layer, the thermal bridge will have no impact on the building's energy consumption. The value of

the thermal bridge of the openings depends on the length from the load-bearing layer and the mounting place of the window, and on the materials used to mount the window, such as installing foam, framework, fasteners and finishing elements. The longer the length between the wall and the window, the higher the required number of anchor brackets attached directly to the window frame and the outer wall retaining layer. However, point thermal bridges (PTB) appear at the points where the anchor brackets are attached. Thus, using a lot of them is not efficient.

Anchor holders are often made of plastic, which has a much lower thermal conductivity value than metal, to reduce energy loss due to point thermal bridges. However, the support force of this type of bracket has drawbacks: plastic is flexible. It may not withstand heavy high-performance windows in the thermal insulation layer that have a greater length than the load-bearing layer. The weight of the opening parts of such glass systems is a minimum of 130 kg. Therefore, only steel brackets, whose thermal transmittance value is $50 \text{ (W/(m}\cdot\text{K))}$, are suitable for installing windows in passive houses. This means the material of anchor brackets has a huge impact on the efficiency of high-energy-performance buildings. To assess the real energy consumption, buildings must evaluate the additional heat losses due to PTB. Otherwise, the energy efficiency calculations for the building might be incorrect.

Designers and builders are looking for new ways to reduce the impact of PTB on a building's energy costs [29]. A new method for installing windows in a thermal insulation layer is currently being applied in practice. A prefabricated frame, made of higher-density stone wool boards (SWB) and auxiliary elements, is being used for the installation of window frames (Figure 3). Practice shows that such window installation is not complicated due to the lightness of the thermal insulation board and the simplicity of the fastening elements. Moreover, it is suitable for installation on any retaining wall, and the thermal conductivity of the frame made of thermal insulation material is low. Such a frame's static properties are sufficient for installing a high-performance window up to 350 mm away from the retaining wall layer. Since metal fasteners do not connect, it is unlikely to create a PTB effect. However, installing windows in this way is little studied compared to the general thermal research context. Therefore, this work aims to investigate the thermal properties of windows installed in the thermal insulation layer in detail and to compare different installation methods and thermal bridge evaluation methodologies from the point of view of thermal physics.

A major concern regarding the design and manufacturing of advanced windows is related to their sound insulation performance. Recent studies have demonstrated the effectiveness of porous absorbent materials in the cavity perimeter of windows [30], as well as the effect of ventilation-enabling façade noise control devices for congested high-rise cities [31]. Active noise control, which uses a secondary sound to cancel unwanted noise, has been successfully implemented and is considered to be an established technique for enhancing the sound insulation of windows [32].

2. Methodology

2.1. Research Object

The schemes of the investigated wall structure and the window frame are given in Figure 3. Additionally, the values of the layer's thickness and thermal conductivity coefficient are shown in the same figure. Accordingly, the heat transfer coefficient of the wall structure is $U = 0.12 \text{ W/(m}^2\cdot\text{K)}$.

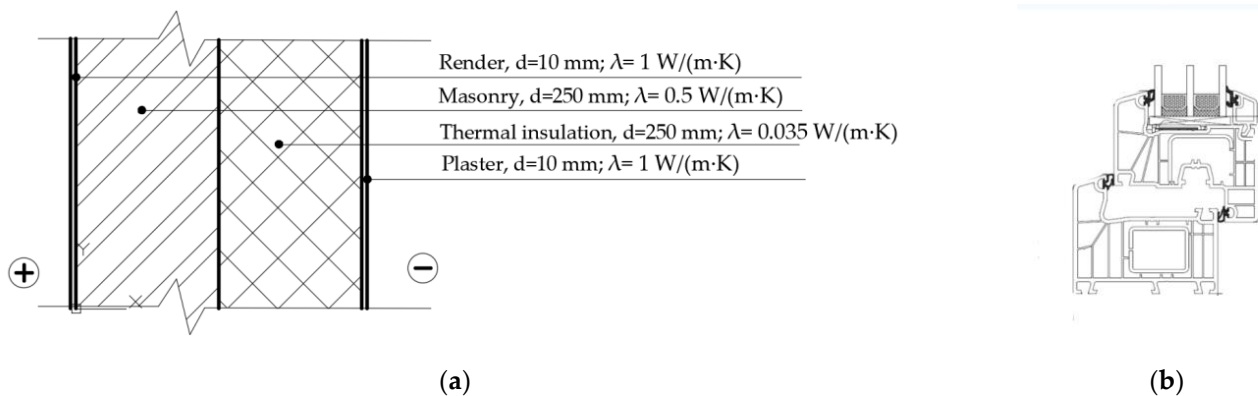


Figure 3. The scheme of the investigated wall structure (a) and of the investigated window frame (b).

The wooden frame of the analyzed window consists of 6 chambers, and its thickness is 100 mm. The value of the thermal conductivity coefficient $\lambda = 0.13 \text{ W}/(\text{m}\cdot\text{K})$. The calculations were simplified and the heat exchange over the glass area was not detailed.

The installation of a window on the wall's opening using stone wool boards (SWB) was chosen for the study (Figure 4). The thermal conductivity coefficient of the special rigid SWB is $\lambda = 0.059 \text{ W}/(\text{m}\cdot\text{K})$. The window frame fastener W length is 192 mm; width—50 mm; wall thickness—2 mm; thermal insulation thickness—48 mm. The length of the corner fastener CL of the thermal insulation panels (when the thickness of the thermal insulation layer was $> 200 \text{ mm}$) is 192 mm; width—192 mm (respectively 96 mm on one side of the corner); wall thickness—2 mm. The thermal insulation board interconnect EL length was 192 mm; width—192 mm; wall thickness—2 mm. The investigation evaluated two wall installation fasteners measuring $80 \times 100 \text{ mm}$. The calculations estimated one wall installation fastener measuring $80 \times 100 \text{ mm}$. This method of installation does not require gaskets, as the thermal insulation material is flexible and allows the window frame to be installed tightly.

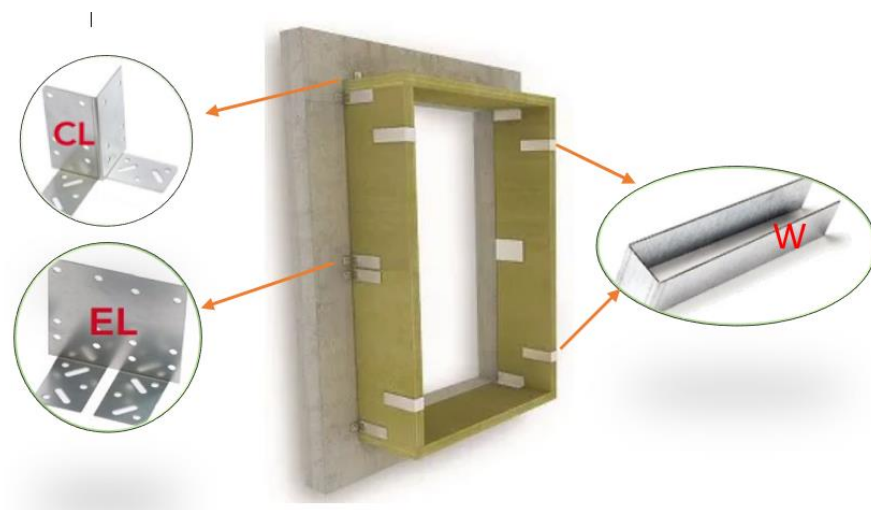


Figure 4. System of window installation in the insulation layer using the stone wool boards (SWB) REDAir TM LINK [33].

2.2. Thermal Bridge Evaluation Methodology

Regarding the evaluation of the thermal bridges, the standard EN ISO 14683:2017 [34] presents three different methodologies:

- Numerical simulation (3-D);
- Choosing from catalogues and atlases;

- Calculation under steady-state conditions (2-D).

This study was guided by methodologies 1 and 3, as this work investigated a new way of connecting windows using SWB. The thermal bridge values of such a connection between a window and the walls have not been studied so far. Therefore, these values are not given in catalogues.

Thermal bridges may be defined according to EN ISO 10211: 2017 [9]. The calculation scheme is given in Figure 5.

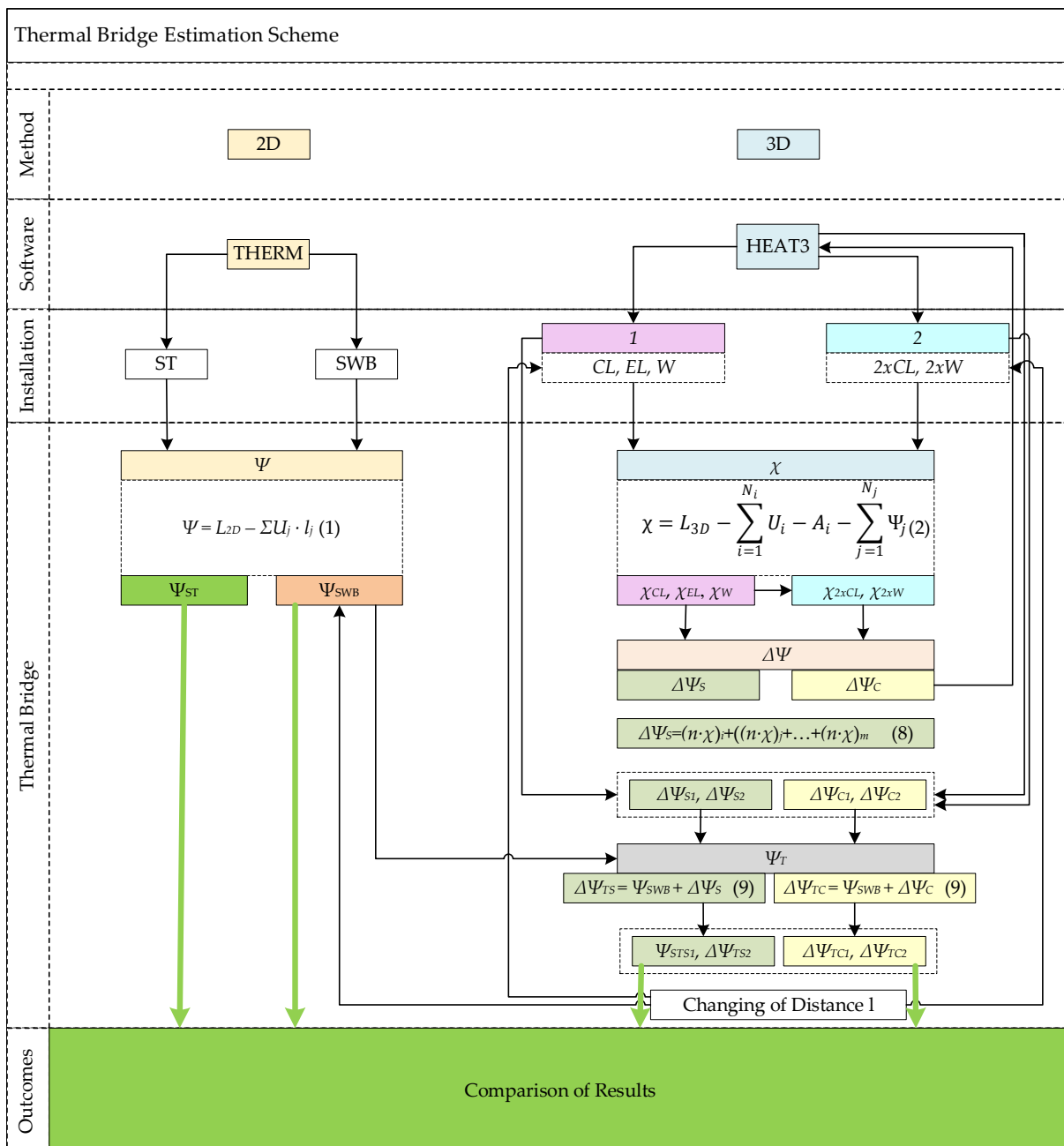


Figure 5. Thermal bridge estimation scheme (prepared by the authors based on [35]).

The LTB around the openings was calculated using the 2-D software THERM [36]. This method is based on the 2-D dimensions. The heat flow moves horizontally in the x-

and y -axis directions. The linear thermal transmittance of the thermal bridges (Ψ) was calculated according to Equation (1):

$$\Psi = L_{2D} - \sum U_j \cdot l_j \quad (1)$$

where L_{2D} is the linear thermal coefficient obtained by calculating the 2-D component for the two environments considered; U_j is the thermal transmittance of the 1-D component j separating the two environments being considered; l_j is the length within the 2-D model applied in the value of U_j .

At the beginning of the study, the LTB was calculated for installation of the window in a load-bearing layer without innovative installation elements and additional insulation; thus, standard Ψ_{ST} . The Ψ_{SWB} of the window opening with an SWB was determined in parallel using the same calculation method. Metal fasteners were not considered at this stage of the calculation.

To evaluate the influence of fasteners on heat loss through the window opening edge, the software HEAT3 [37], with a 3-D temperature field calculation, was used in this study.

For installing windows in the cross-section of thermal insulation material, various fasteners are used, and their influence on heat loss can be assessed by point thermal transmittance χ , $W/(m \cdot K)$. The point thermal transmittance (value— χ) was calculated as in Equation (2):

$$\chi = L_{3D} - \sum_{i=1}^{N_i} U_i - A_i - \sum_{j=1}^{N_j} \Psi_j \quad (2)$$

where L_{3D} is the linear thermal coefficient obtained by calculating the 3-D component for the two environments considered; U_j is the thermal transmittance of the 1-D component I separating the two environments considered; A_i is the area applied in the value U_i ; Ψ_j is linear thermal transmittance; l_j is the length which the value of Ψ_j applies; N_j is the number of 2-D components; N_i is the number of 1-D components.

The partial differential equation is replaced by a discrete approximation in the numerical formulation. Values at discrete points are used to approximate the temperature field. A computational mesh is created because of this. Δx_i , Δy_j , and Δz_k , are the increments in the x -, y -, and z -directions, respectively [38].

A cell (i, j, k) with the side lengths Δx_i , Δy_j , and Δz_k is shown in Figure 6. Figure 6 also indicates $(i, j, k+1)$ directly above the cell. There are six cells next to each other.

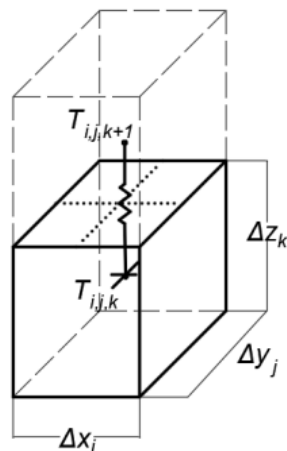


Figure 6. Computational cells (i, j, k) and $(i, j, k+1)$ [38].

The heat flow $Q_{i,j,k+1/2}$ (W), from cell (i,j,k) to cell $(i,j,k+1)$ is given by the thermal conductance multiplied by the temperature difference between these two cells (Equation (3)):

$$Q_{i,j,k+1/2} = K_{i,j,k+1/2} \cdot (T_{i,j,k} - T_{i,j,k+1}) \quad (3)$$

where $K_{i,j,k+1/2}$ is the conductance between the two cells (i,j,k) and $(i,j,k+1)$, W/K; $(T_{i,j,k} - T_{i,j,k+1})$ is the temperature difference between the two cells.

The other five heat flows pertaining to cell (i,j,k) are calculated correspondingly.

Figure 7 shows the six-thermal conductance of cell (i,j,k) . The conductance $K_{i,j,k+1/2}$ (W/K), between the two cells (i,j,k) and $(i,j,k+1)$ is calculated as [38]:

$$K_{i,j,k+1/2} = \frac{\Delta x_i \cdot \Delta y_i}{\frac{\Delta z_k}{(2 \cdot \lambda_{i,j,k})} + \frac{\Delta z_{k+1}}{(2 \cdot \lambda_{i,j,k+1})} + R_{i,j,k+\frac{1}{2}}} \quad (4)$$

where $\lambda_{i,j,k}$ is the thermal conductivity in cell (i,j,k) , W/(m·K); $(\Delta x_i \cdot \Delta y_i)$ is the conductance refers to the total heat flow through the area, m; Δz_k is the z-direction for half of the cell (i,j,k) ; $R_{i,j,k+1/2}$ is an optional additional thermal resistance at the interface between the two cells (i,j,k) and $(i,j,k+1)$, (m²·K/W).

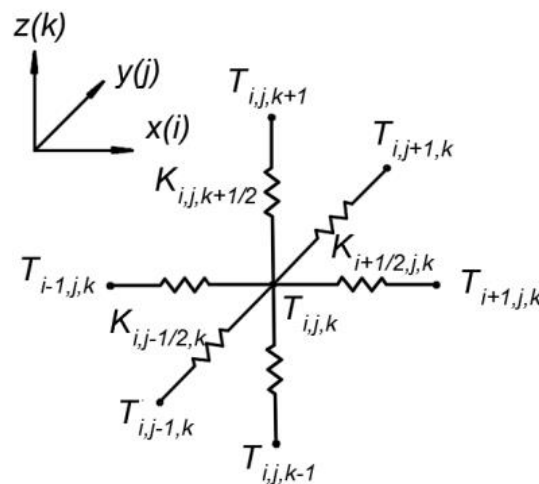


Figure 7. Thermal conductance connected to cell $(i; j; k)$ [38].

The thermal resistance in the z-direction for half of the cell (i,j,k) is the first term in the denominator, and the resistance for half of the cell $(i,j,k+1)$ is the second term. $R_{i,j,k+1/2}$ is an optional extra thermal resistance at the interface between the two cells (i,j,k) and $(i,j,k+1)$.

Equation (4) is valid for all internal cells (an internal cell has at least one cell on each side). For boundary cells, the Equation (4) was modified in the following way. Consider cell $(1,j,k)$, which lies at a boundary. The conductance that couples the temperature $T_{1,j,k}$ with a boundary temperature is as shown in Equation (5):

$$K_{\frac{1}{2},j,k} = \frac{\Delta y_j \cdot \Delta z_k}{\frac{\Delta x_1}{(2 \cdot \lambda_{1,j,k})} + R_{\frac{1}{2},j,k}} \quad (5)$$

where $R_{1/2,j,k}$ is the boundary surface resistance, (m²·K/W).

An energy balance is made for each cell. The total heat flow to cell (i, j, k) from the six adjacent cells is put in the variable $H_{i,j,k}$, (W) (Equation (6)):

$$H_{i,j,k} = K_{i-\frac{1}{2},j,k} \cdot (T_{i-1,j,k} - T_{i,j,k}) + K_{i+\frac{1}{2},j,k} \cdot (T_{i+1,j,k} - T_{i,j,k}) + K_{i,j-\frac{1}{2},k} \cdot (T_{i,j,k-1} - T_{i,j,k}) + K_{i,j+\frac{1}{2},k} \cdot (T_{i,j,k+1} - T_{i,j,k}) + K_{i,j,k-\frac{1}{2}} \cdot (T_{i,j,k-1} - T_{i,j,k}) + K_{i,j,k+\frac{1}{2}} \cdot (T_{i,j,k+1} - T_{i,j,k}) \quad (6)$$

For a more quantitative comparison later, the average point thermal transmittance $\bar{\chi}$, $W/(m \cdot K)$, was calculating using Equation (7):

$$\frac{\int_a^b \chi dl}{b-a} \quad (7)$$

where a —starting position; b —end position; χ —point thermal transmittance as a function of length from the masonry layer. In practice, the latter is determined by fitting a function over the graph.

At this stage of the calculation, two cases of window frame installation in SWB were analyzed (Figure 5):

1. A part of the wall 1 m high and with three fasteners: corner fastener CL, interconnect fastener EL, and window fastener W (Figure 4). The values χ_{CL} , χ_{EL} , χ_{W4} were determined;
2. A part of the wall 1 m high and with two corner fasteners CL and two window fasteners W (Figure 4). The values $\chi_{2 \times CL}$, $\chi_{2 \times W}$ were determined.

The supplement $\Delta\Psi$ to the value of the LTB was evaluated in two ways:

The supplement of the total linear thermal bridge $\Delta\Psi_S$ of the separate fasteners was calculated according to Equation (8):

$$\Delta\Psi_S = (n \cdot \chi)_i + ((n \cdot \chi)_j + \dots + (n \cdot \chi)_m) \quad (8)$$

where n —average number of fasteners per meter of opening; i, j, \dots, m —different types of metal fasteners.

The supplement $\Delta\Psi_C$ of the LTB was calculated comprehensively for all fasteners used in the calculation. These results were provided by the HEAT3 computer program.

Thus, the total Ψ_T of the thermal bridges using SWB and metal fasteners was calculated from Equation (9):

$$\Psi_T = \Psi_{SWB} + \Delta\Psi \quad (9)$$

An analysis was also performed showing how the values of thermal bridges were distributed by changing the installation place of the window in the thermal insulation layer. Changing the place of the window installation was evaluated in the calculation. A value of 0 mm means that the window is mounted next to the edge of the load-bearing layer, and a value of 150 mm means that the window is installed right outside the wall (thermal insulation layer). Therefore, 75 mm denotes the middle of the thermal insulation layer (Figure 8). The values of the longitudinal thermal bridge in the thermal insulation layer were calculated starting from a value of 0 by adding 10 mm towards the outer side of the barrier, i , from $0 + 10_i + 10_j \dots + 10_n = 150$ mm.

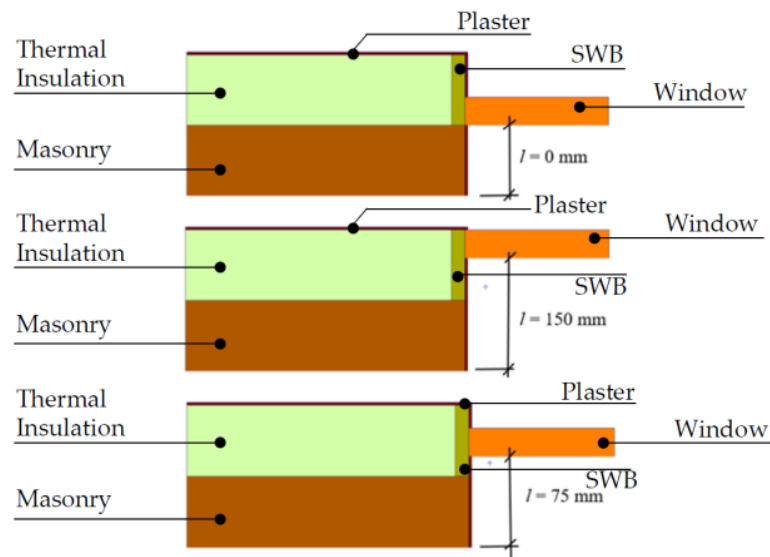


Figure 8. Schema of basic positions of the window frame in the section of the thermal insulation layer using SWB.

3. Results

3.1. Linear Thermal Bridges at Window Openings without Considering the Influence of Metal Fasteners

The results of the study show that the thermal bridge through the standard installation site (old building, without insulating the window frame with SWB) gives a transmittance of $\Psi_{ST} = 0.13 \text{ W}/(\text{m}\cdot\text{K})$, while using SWB for window framework insulation, the value of the thermal bridge transmittance is $\Psi_{SWB} = 0.026 \text{ W}/(\text{m}\cdot\text{K})$. The difference between these values is 80%.

By analyzing the dependence of the LTB on the window installation length in the thermal insulation material, the obtained results show (Figure 9) that the lowest value Ψ_{SWB} is obtained when the window-mounted place is at a distance of 70–80 mm from the load-bearing layer. The thermal transmittance average slowly increases, moving along the thermal insulation layer to the edge of the load-bearing layer.

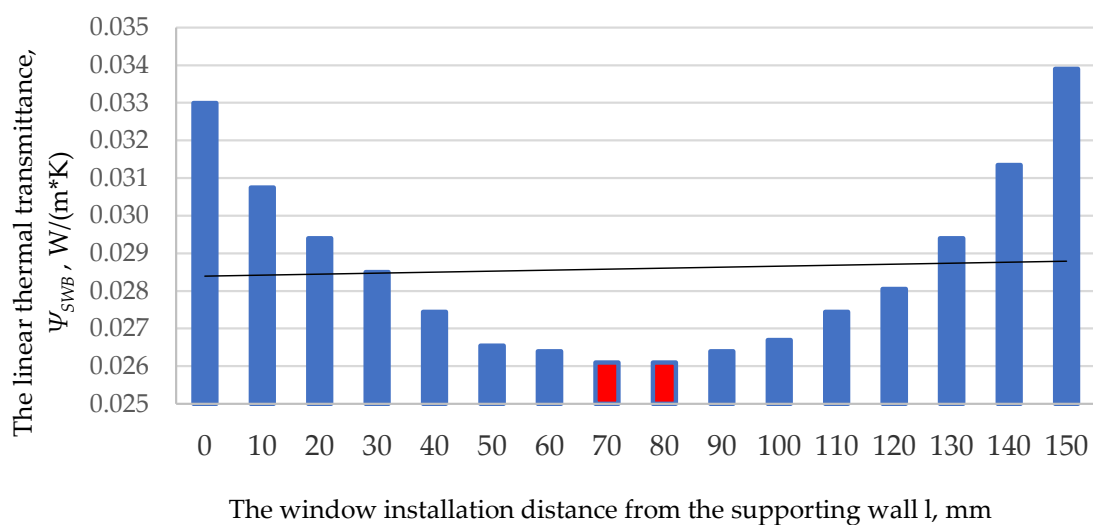


Figure 9. Dependence of the value of thermal transmittance on the installation length in SWB from the place of window to the load-bearing layer.

3.2. Thermal Bridges by Assessing the Influence of Metal Fasteners

3.2.1. Point Thermal Bridges

A computer simulation was performed to evaluate the influence of metal fasteners on the heat loss of the building. The results (Figure 10) show that $\chi_{CL} = 0.0114 \text{ W}/(\text{m}\cdot\text{K})$; $\chi_{EL} = 0.0225 \text{ W}/(\text{m}\cdot\text{K})$ and $\chi_w = 0.0181 \text{ W}/(\text{m}\cdot\text{K})$ when the mounting place of the window is 100 mm from the supported wall.

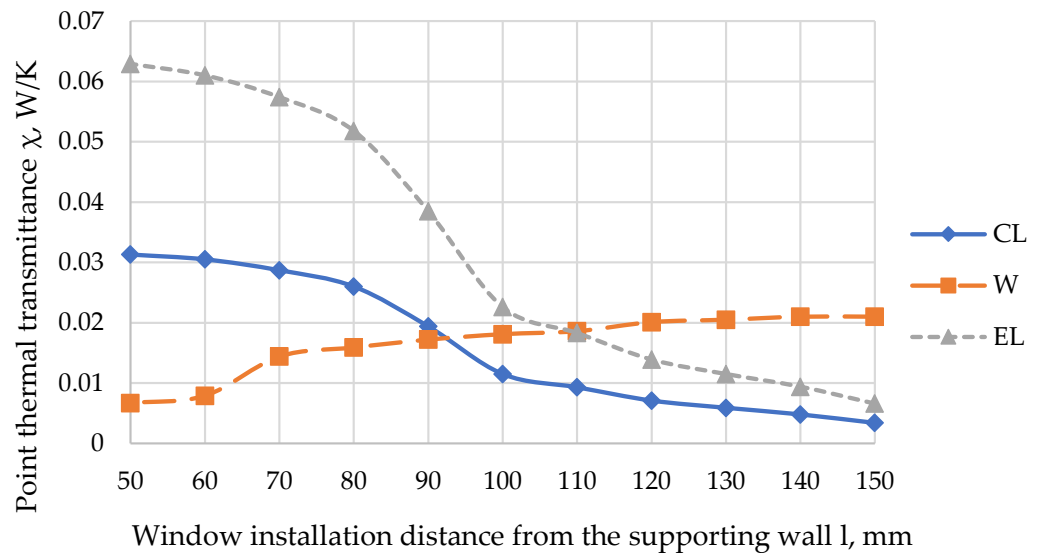


Figure 10. Dependence of the values of PTB on the window installation distance from the load-bearing layer edge for individual window mounting elements CL, EL, W.

By assessing how the values of the χ_{CL} , χ_{EL} , χ_{W48} depend on the distance between the window installation and the edge of the load-bearing layer wall for separate window mounting elements CL, EL, W, the research results (Figure 10) show that using corner fastener CL and interconnect fastener EL, the PTB is the highest at a distance of 50–100 mm from the load-bearing layer ($\chi_{CL} = 0.0313 \text{ W}/(\text{m}\cdot\text{K})$ and $\chi_{EL} = 0.0629 \text{ W}/(\text{m}\cdot\text{K})$). Meanwhile, the lowest values are obtained when $l = 150 \text{ mm}$ ($\chi_{CL} = 0.0034 \text{ W}/(\text{m}\cdot\text{K})$ and $\chi_{EL} = 0.00606 \text{ W}/(\text{m}\cdot\text{K})$). However, analyzing the PTB of fastener W, the results are the opposite. As the length l (length between the installed window framework and the load-bearing layer) decreases, the value of the PTB decreases, with a maximum value $\chi_W = 0.021 \text{ W}/(\text{m}\cdot\text{K})$ and minimum $\chi_W = 0.0067 \text{ W}/(\text{m}\cdot\text{K})$ at $l = 150 \text{ mm}$ and $l = 50 \text{ mm}$, respectively.

In addition, the average value of χ was calculated for each fastener. The results were $\chi_W = 0.0168 \text{ W}/(\text{m}\cdot\text{K})$, $\chi_{CL} = 0.0161 \text{ W}/(\text{m}\cdot\text{K})$ and $\chi_{EL} = 0.0319 \text{ W}/(\text{m}\cdot\text{K})$. Thus, on average, the interconnect fastener EL has twice the thermal transmittance as the corner fastener CL.

3.2.2. The Supplement of the Linear Thermal Bridges

The calculation of LTB's supplement was performed in two ways: 1 case summing the χ of separate fasteners (Figure 11b,c) (in this case, the value of LTB's supplement was found to be $\Delta\Psi_{s1} = 0.0521 \text{ W}/(\text{K}\cdot\text{m})$), and 2 case HEAT3 software provided the value of all three investigated fasteners in combination (Figure 11a). The described value of LTB's supplement was determined for separate fasteners (the 1 case in Figure 5). In this case, LTB's supplement's value was lower, and was equal to $\Delta\Psi_{c1} = 0.0515 \text{ W}/(\text{K}\cdot\text{m})$.

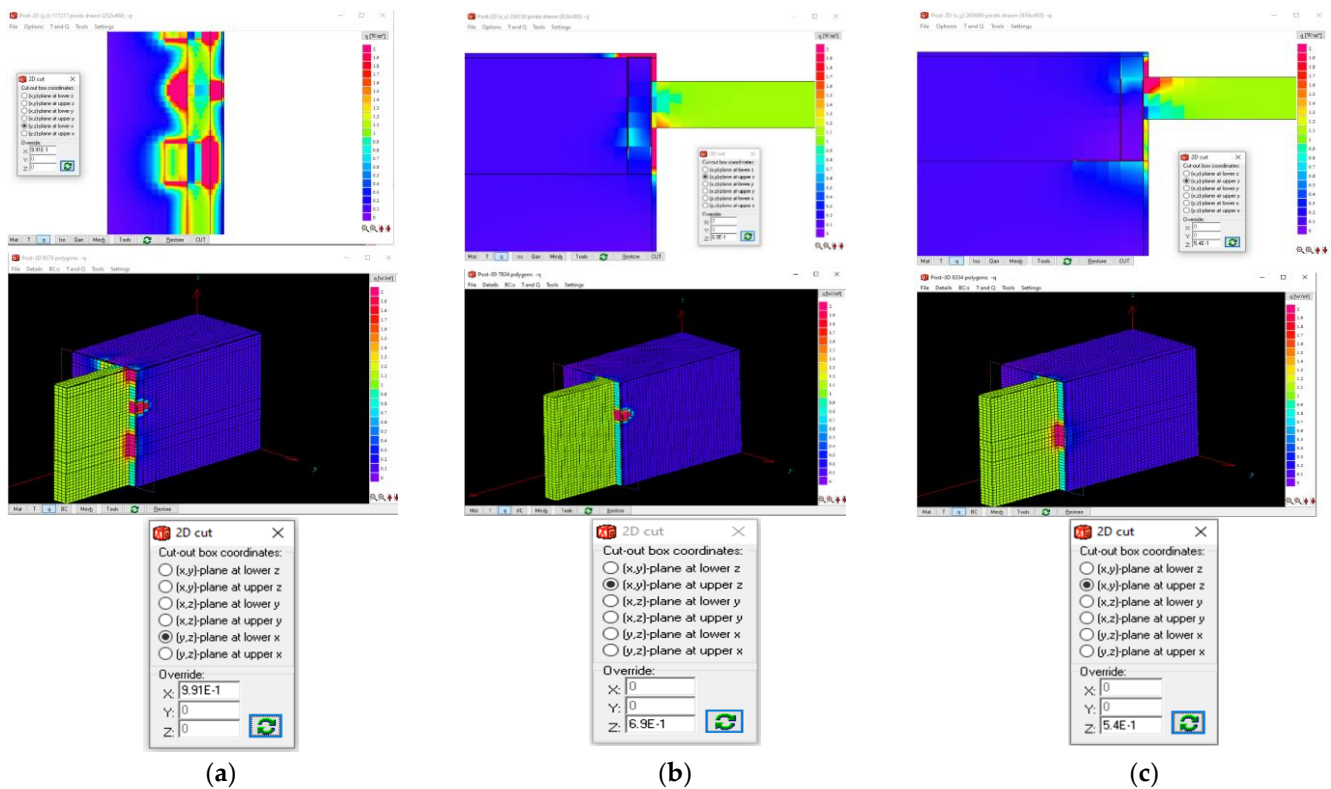


Figure 11. Intensity of heat flows in the cross-section of fasteners: (a) set of fasteners: corner fastener CL, interconnect fastener EL, and window frame fastener W; (b) separate W fastener; (c) separate EL fastener.

Analyzing the 2 case (Figure 5), involving an opening edge 1 m long with $2 \times CL$ and $2 \times W$, it was found that when evaluating the influence of four metal elements in a combination (calculation option 2), supplement heat loss through this element was $\Delta\psi_{c2} = 0.0591 \text{ W}/(\text{K}\cdot\text{m})$. After summing (calculation option 1) the point thermal bridges of separate fasteners ($2 \times CL$ and $2 \times W$), the supplement of the linear thermal bridges was $\Delta\psi_{s2} = 0.0592 \text{ W}/(\text{K}\cdot\text{m})$.

3.2.3. Total Linear Thermal Bridge

The results reveal that the sum of the separate fasteners' total linear thermal transmittance value is $\psi_{TS1} = 0.0781 \text{ W}/(\text{K}\cdot\text{m})$. A similar result $\psi_{TC1} = 0.0775 \text{ W}/(\text{K}\cdot\text{m})$ was obtained using the HEAT3 software, where the influence of the combination of metal fasteners was assessed.

In the case using $2 \times CL$ and $2 \times W$, the total thermal transmittance was found to be $\psi_{TS2} = 0.0852 \text{ W}/(\text{K}\cdot\text{m})$ (considering metal fasteners separately) and $\psi_{TC2} = 0.0852 \text{ W}/(\text{K}\cdot\text{m})$ (assessing the influence of the combined metal fasteners).

3.3. Comparison of the Values of Thermal Bridges Analyzed by Different Calculation Methods

A comparison of the values of all LTB analyzed in this study is presented in Figure 12. The study results show that the thermal bridge through the standard installation site (old building, without insulating the window frame with SWB) gives a transmittance of $\psi_{ST} = 0.13 \text{ W}/(\text{m}\cdot\text{K})$. Meanwhile, using SWB for window framework insulation, the value of the thermal bridge transmittance is $\psi_{SWB} = 0.026 \text{ W}/(\text{m}\cdot\text{K})$. The difference between these values is 80%. However, after estimating the metal fasteners, the difference is 37%.

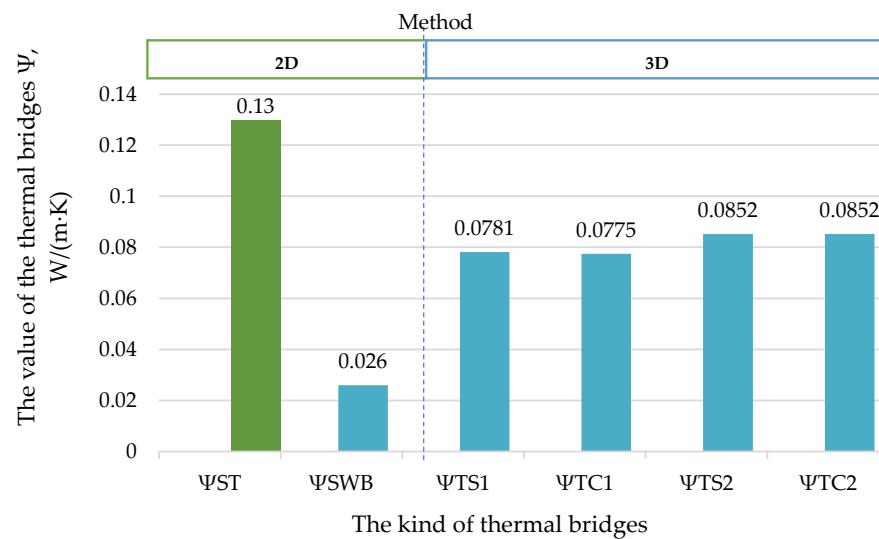


Figure 12. Comparison of the values of thermal bridges analyzed using different calculation methods.

If we compare the calculation results according to different methodologies, it can be seen that when the window is mounted into the load-bearing layer ($l = 0$ mm), the results of the total thermal bridge ($\Psi_{TS1} = 0.0781$ W/(m·K); $\Psi_{TS2} = 0.0852$ W/(m·K)) are almost the same (difference 0.8% and 0%) as those for the complex thermal bridge ($\Psi_{TC1} = 0.0775$ W/(m·K); $\Psi_{TC2} = 0.0852$ W/(m·K)); therefore, the calculation results according EN ISO 10211: 2008 [9] differ fractionally from the results provided by the HEAT3 program.

However, when assessing changes in the mounting place of the window in the thermal insulation layer, a discrepancy appears between the results of the different methodologies used. In this study, the distribution of the value of Ψ_T was analyzed by changing the window installation location in the thermal insulation layer and using different calculation methods to determine the supplement thermal bridge values: complex $\Delta\Psi_C$ (calculation option (2)) and summed $\Delta\Psi_S$ (calculation option (1)). The results (Figure 13) reveal that the summing values of the supplement thermal bridge ($\Delta\Psi_{S2}$) of $2 \times CL$ and $2 \times W$ may vary from 26.2% to 40.9% compared to the complex values $\Delta\Psi_{C2}$ used in the same calculations performed by the HEAT3 program. The thermal bridge values depend on the mounting location in the opening in terms of distance from the load-bearing layer. The trends indicate that the further away from the load-bearing layer, the bigger the difference between the thermal bridge values determined by different methods.

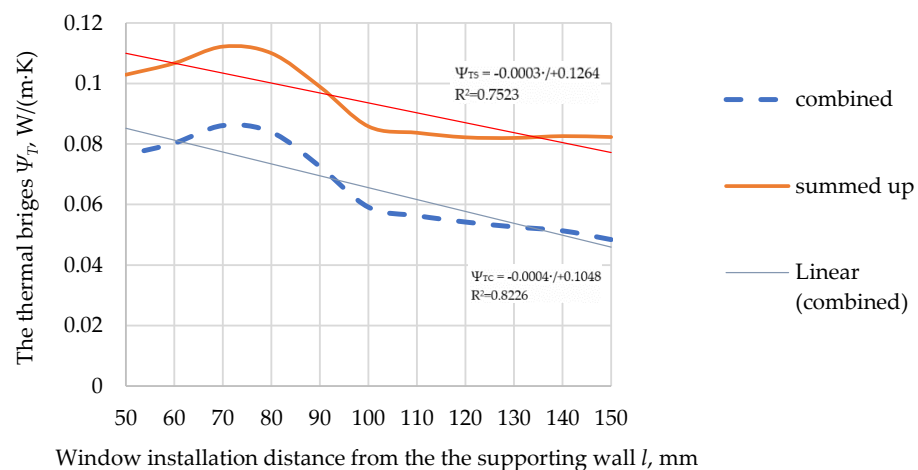


Figure 13. Dependence of the Ψ_T value of the thermal bridge on the distance of the window installation from the load-bearing layer edge and calculation method.

The results (Figure 13) also show that in the calculations, applying the summing (calculation option (1)) of thermal bridge values ($\Delta\Psi_{S2}$) and the value of thermal bridges of the window mounted in the thermal insulation layer at a length of 50–100 mm from the load-bearing layer was 28% greater than the window mounted in the span of 100–150 mm. The highest value of the thermal bridge ($\Psi_{TS2} = 0.1122$, W/(m·K)) was at a length of 70 mm from the load-bearing layer, and the lowest value of Ψ_{TS2} (0.0820, W/(m·K)) was at a length of 130 mm from the load-bearing layer.

The results (Figure 13) show that by applying $\Delta\Psi_{C2}$ (calculation option (2)) and mounting the window at a length of 50–100 mm from the load-bearing layer, the values of thermal bridges increased by 30% compared to the values of thermal bridges at a distance of 100–150 mm from the load-bearing layer. The highest value of the thermal bridge ($\Psi_{TC2} = 0.0861$, W/(m·K)) was at 70 mm from the load-bearing layer, and the lowest value of Ψ_{TC2} (0.0484, W/(m·K)) was at a length of 150 mm from the load-bearing layer.

4. Discussion

To meet the EU's goals of creating a sustainable, competitive, secure, and decarbonized energy system by 2050, the EU is stepping up the renovation process to turn old buildings into NZEB. Following Directive (EU) 2018/844 [3], the renovation of old buildings will mainly focus on renewable sources. However, important issues remain, namely, the insulation of the building envelope, the modernization of HVAC, and similar [22,39,40]. This work focused on the subtleties of installing new high-performance windows, which will ensure high energy efficiency, sufficient air thickness, and a comfortable indoor microclimate. Several assumptions have been made in analyzing this problem, such as that installing a window in a thermal insulation layer results in a zero thermal bridge or those metal fasteners have a negligible effect on thermal transmittance. However, the investigation has shown that these two assumptions were incorrect. A certain value of the thermal bridge of the opening edge is usually obtained due to the difference in the thickness of the window and wall structures and the different materials used at the window installation site.

The authors of this study analyzed the installation of windows using SWB. The study results revealed that the insulation of the window frame was a very important issue related to the energy consumption of the building. By insulating the window frame with SWB, it was possible to reduce the value of the thermal bridge at the junction of the wall and the window framework by 80% (but not 100%). Meanwhile, other researchers who have examined the issue of the thermal bridge of the window opening have stated that for some cases, placing the window in the most energy-efficient position reduces the linear thermal transmittance by more than 50% [41].

This excellent 80% result due to the heat saving of the building is given by the 2-D calculation method when neglecting the fasteners used in the installation scheme that are used for fastening a special thermal insulation board to the masonry and the window. It is always an important question what influence the attachment of metal elements (various bolts, etc.) to the load-bearing structure and each other has on the evaluation of thermal bridges. The study showed that using SWB and considering the metal reinforcement details reduces the value of the thermal bridge by up to 37% compared to the standard without the insulation option. In this case, the metal elements closer to the warm and cold partition sides do not come into contact, so there is no continuous heat flow through the metal elements.

The maximum value of χ was achieved for the fastener W. In practice, the middle fastener W, which is used to join the insulation boards, may be missing if the window is not large, because the length of the insulation boards is 1500 mm. Therefore, if the window dimension is less than 1400 mm, no joining of the panels will be required, which means that the parts will need W either. Therefore, the total value of the thermal bridge will change significantly.

Analysis of the different calculation methods revealed a 0.8% difference between 2-D (calculation according to EN ISO 10211: 2017) and 3-D (numerical simulation with HEAT3).

Comparing calculation options of the composite (2) and summing (1) models of evaluation of the thermal bridge with the fasteners $2 \times CL$ and $2 \times W$ at a length of 1 m, the opening edge showed no difference between the results. However, the study results showed that different calculation methodologies could significantly skew the results if the length from the load-bearing layer assesses. As the window mount further away from the load-bearing layer, the thermal bridge values difference due to using the different methods is bigger. Calculating the total thermal bridge regarding summing model of separate fasteners ($\Delta\Psi_{S2}$) might change the results by 26% to 41% compared to the same calculations using composite model ($\Delta\Psi_{C2}$), calculated by the HEAT3 program. The above-mentioned appears because the heat flows of these fasteners interact with each other, even though a large thermal insulation layer allocates these fasteners. Therefore, it would be appropriate to evaluate the PTB of each fastener separately. It would also be easy to estimate the additional heat loss through the opening edge of any particular window by having PTB for the individual elements and a mounting scheme for any window. However, it is very difficult to assess these small fasteners properly, as they can vary greatly in dimensions (length, cross-section), numbers (depending on loads, base, technological requirements) and the materials to which they are attached (different bases). Therefore, the calculations may differ from case to case.

3-D thermal numerical simulation is required to estimate the influence of metal fasteners on heat loss accurately. This study shows that evaluating the composite model of these fasteners (using HEAT3) results in a lower additional heat flux compared to the total heat fluxes of the summing of separate fasteners. However, to properly assess the influence of metal fasteners, the composite thermal bridge model should be calculated using the 3-D calculation method for each window according to a separate installation scheme. For designers, such a calculation method would become a serious challenge because, without special software, it is impossible to do so. Therefore, in the frequent case of assessing the energy performance of a building, the second assumption is made not to evaluate metal fasteners and to limit oneself to the 2-D calculation method.

The authors compared the obtained values of the thermal bridge by using the 2-D and 3-D calculation methods, and the calculation results using a 2-D environment showed that $\Psi_{SWB} = 0.026 \text{ W}/(\text{m}\cdot\text{K})$, while in the 3-D environment, this value was accordingly, $\Psi_T = 0.0815 \text{ W}/(\text{m}\cdot\text{K})$. The difference was 68%. From the results of this study, one can conclude that by ignoring PTB and using metal elements for window mounting, a significant difference can be obtained between the calculated (2-D method) and the expected real heat loss (3-D method). This fact is confirmed by other scientists [42].

Additionally, comparing 2-D and 3-D calculation methodologies, the arrangement of thermal bridge values by length l took the opposite trend (Figure 7). In the 2-D temperature field, the thermal bridge values were lowest when the window was installed in a layer of thermal insulation material at a distance of 70–80 mm from the load-bearing layer $\Psi_{SWB} \approx 0.026 \text{ W}/(\text{K}\cdot\text{m})$. The results presented in Figure 9 show that with increasing length l , the value of the thermal bridge also increased. Similar results have been obtained by other researchers [11,17,43]. Ilomets et al. [44] state that insulating the walls of an existing building with a > 200-mm-thick layer of thermal insulation increases the value of the thermal bridge at the window opening by 34%. The authors mentioned above investigated cases where metal parts were fixed directly to the load-bearing layer or brackets. Meanwhile, the values of thermal bridges calculated by the 3-D method were distributed with the opposite trend: as the length l increased, the thermal bridge values decreased. This can be explained by the fact that when using SWB, metal fasteners do not cross the layer of thermal insulation material directly and do not come into contact with each other—they do not act as direct heat conductors. Therefore, it is risky to evaluate thermal bridges only using the 2-D methodology when designing energy-efficient buildings.

In addition, looking at the results shown in Figure 14, an interpolation of the curves can be performed to deduce the crossing point of both graphs. In this case, both curves cross at around 180 mm with $0.0408 \text{ W}/(\text{K}\cdot\text{m})$. It follows that there is no difference between

2-D and 3-D methodologies around that point. Thus, metal fasteners do not affect the window's overall thermal performance.

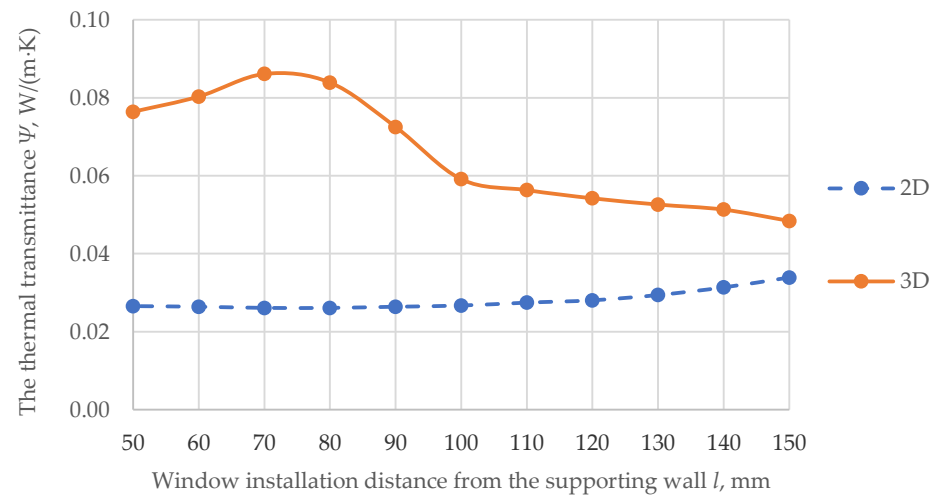


Figure 14. Trends in the values of thermal bridges due to the change of the installation location in the layer of thermal insulation material, applying different calculation methodologies.

The linear thermal transmittance of the NZEB must be a maximum of $0.05 \text{ W}/(\text{K}\cdot\text{m})$ according to the Lithuanian national document STR 2.01.02: 2016 [20]. The results (Figure 15) show that if thermal bridges are evaluated using the 2-D method, i.e., without considering metal fasteners, then the solution for window mounting using SWB always complies with the requirements of STR. If one considers metal fasteners, the window must be installed no closer than 100 mm from the retaining wall for the value of the thermal bridge at the window opening to meet the requirements of STR (Figure 15). The study results show that the installation position of the window in the layer of thermal insulation material is a very important issue. The results show that in NZEB buildings where the wall insulation layer is greater than 200 mm, the windows need to be mounted using SWB. This installation method ensures the lowest thermal bridges and sufficient static loads by extending the window frame into the thermal insulation layer at a length of more than 100 mm from the retaining wall. The farther from the retaining wall, the smaller the thermal bridge. It has been mentioned earlier that other methods of installing windows show the opposite results, which makes it difficult to ensure the status of an NZEB when using such mounting methods.

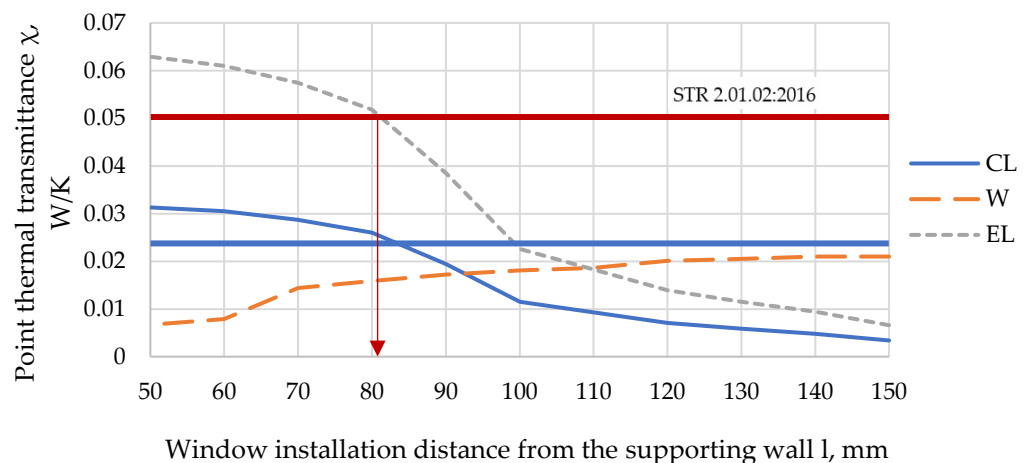


Figure 15. Compliance of the linear thermal transmittance of the investigated metal fasteners with the normative requirements.

This study focused on only one method of window installation using SWB. This preliminary study has given rise to a focus on ever-improving design solutions. This construction progress is influenced by energy policy, forcing us to rethink whether we are evaluating the energy efficiency of buildings or whether the standardized values for thermal bridges in the atlases are inappropriate. Therefore, from a prospective point of view, it would be possible to investigate other window installation types proposed in several atlases or in passive houses, thus providing solutions with extremely low thermal bridging effects.

5. Conclusions

This work is another small step towards improving the assessment of the energy performance of a building. Examining the method of installing a new high-performance window in a thermal insulation layer is important for highlighting the effect of installing a window on the wall of a building. Given that windows are the most thermally conductive elements in a building, this paper guides both the scientific community and practitioners on trends in thermal bridges that are completely changing using different assessment methods.

Comparing the values obtained by using 2-D and 3-D thermal bridge calculation methods, the values show a difference of 68%. The investigation showed that by insulating the window frame with SWB and not evaluating the metal fasteners, we can reduce the value of the thermal bridge at the junction of the wall and the window frame by 80%. However, the evaluation of metal fasteners reduces the thermal bridge value by up to 37% compared to the standard option without insulation.

Furthermore, comparing the results of 2-D and 3-D calculation methodologies, the arrangement of the thermal bridge values according to the length l from the load-bearing layer took the opposite trend. Therefore, it is risky to evaluate thermal bridges only with the 2-D methodology when designing energy-efficient buildings.

Author Contributions: Conceptualization, J.Š., J.R., D.A.K., E.K. and P.A.F.; methodology, J.Š., J.R., D.A.K. and P.A.F.; software, J.Š., J.R., D.A.K. and P.A.F.; validation, J.Š., J.R., D.A.K., E.K. and P.A.F.; formal analysis, J.Š., J.R., D.A.K., E.K. and P.A.F.; investigation, J.Š., J.R., D.A.K. and P.A.F.; resources, J.Š., J.R., D.A.K., E.K. and P.A.F.; data curation, J.Š., J.R., D.A.K., E.K. and P.A.F.; writing—original draft preparation, J.Š., J.R., D.A.K.; writing—review and editing, J.Š., J.R., D.A.K., E.K. and P.A.F.; visualization, J.Š., J.R., D.A.K. and E.K.; supervision, J.Š., J.R., D.A.K. and P.A.F.; funding acquisition, D.A.K. All authors have read and agreed to the published version of the manuscript.

Funding: This research was funded by Poland Ministry of Science and Higher Education, grant number WZ/WB-IIŚ/7/2022.

Acknowledgments: This research was supported by the Basic Science Research Program through the Kaunas Technology University (KTU) and it was carried out as part of a Bialystok University of Technology grant and financed by a research subsidy provided by the minister responsible for science WZ/WB-IIŚ/7/2022. It is a part of Memorandum of Understanding for scientific cooperation between Bialystok University of Technology and Kaunas University of Technology for the years 2021–2026.

Conflicts of Interest: The authors declare no conflict of interest.

References

1. National Energy and Climate Plans (NECPs). European Commission. Available online: https://ec.europa.eu/energy/topics/energy-strategy/national-energy-climate-plans_en (accessed on 27 July 2021).
2. Building Performance Institute Europe (BPIE). *Renovation Strategies of Selected EU Countries. A Status Report on Compliance with Article 4 of the Energy Efficiency Directive*; BPIE: Brussels, Belgium, 2014. Available online: [Renovation-Strategies-EU-BPIE-2014.pdf](https://www.bpie.eu/renovation-strategies-eu-bpie-2014.pdf) (accessed on 1 March 2022).
3. EN. Directive (EU) 2018/844 of the European Parliament and of the Council of 30 May 2018 amending Directive 2010/31/EU on the energy performance of buildings and Directive 2012/27/EU on energy efficiency; the European Parliament and the Council of the European Union. *Off. J. Eur. Union* **2018**, *35*, L156–L175.
4. Building Performance Institute Europe (BPIE). *Future-Proof Buildings for All Europeans*; BPIE: Brussels, Belgium, 2019. Available online: <https://globalabc.org/resources/publications/bpie-future-proof-buildings-all-europeans> (accessed on 1 March 2022).

5. COM/2020/562 Final. Investing in a Climate-Neutral Future for the Benefit of Our People. Communication from the Commission to the European Parliament, the Council, the European Economic and Social Committee and the Committee of the Regions. Stepping up Europe's 2030 Climate Ambition Brussels. Available online: <https://eur-lex.europa.eu/legal-content/EN/TXT/?uri=CELEX%3A52020DC0562> (accessed on 1 March 2022).
6. Renovation Wave | Energy. Available online: https://ec.europa.eu/energy/topics/energy-efficiency/energy-efficient-buildings/renovation-wave_en (accessed on 1 March 2022).
7. Bergero, S.; Cavalletti, P.; Chiari, A. Energy refurbishment in existing buildings: Thermal bridge correction according to DM 26/06/2015 limit values. *Energy Procedia* **2017**, *140*, 127–140. [[CrossRef](#)]
8. O'Grady, M.; Lechowska, A.A.; Harte, A.M. Application of infrared thermography technique to the thermal assessment of multiple thermal bridges and windows. *Energy Build.* **2018**, *168*, 347–362. [[CrossRef](#)]
9. ISO. *EN ISO 10211:2017; Thermal Bridges in Building Construction—Heat Flows and Surface Temperatures—Detailed Calculations*. CEN Committee ISO/TC 163/SC; International Organization for Standardization: Geneva, Switzerland, 2017.
10. Theodosiou, T.; Tsikaloudaki, K.; Bikas, D.; Aravantinos, D.; Kontoleon, K.N. Assessing the use of simplified and analytical methods for approaching thermal bridges with regard to their impact on the thermal performance of the building envelope. In Proceedings of the World SB 14 Conference on the Sustainable Building: Result, Barcelona, Spain, 28–30 October 2014. Available online: http://wsb14barcelona.org/programme/pdf_poster/P-059.pdf (accessed on 1 March 2022).
11. Theodosiou, T.G.; Papadopoulos, A.M. The impact of thermal bridges on the energy demand of buildings with double brick wall constructions. *Energy Build.* **2008**, *40*, 2083–2089. [[CrossRef](#)]
12. Citterio, M.; Cocco, M.; Erhorn-Klutting, H. Thermal bridges in the EPBD context: Overview on MS approaches in regulations. In *ASIEPI Information Paper*. 2008. Available online: https://www.buildup.eu/sites/default/files/P064_EN_ASIEPI_WP4_IP1_p3073.pdf (accessed on 1 March 2022).
13. Evola, G.; Margani, G.; Marletta, L. Energy and cost evaluation of thermal bridge correction in Mediterranean climate. *Energy Build.* **2011**, *43*, 2385–2393. [[CrossRef](#)]
14. Martin, K.; Escudero, C.; Erkoreka, A.; Flores, I.; Sala, J.M. Equivalent wall method for dynamic characterization of thermal bridges. *Energy Build.* **2012**, *55*, 704–714. [[CrossRef](#)]
15. Gao, Y.; Roux, J.J.; Zhao, L.H.; Jiang, Y. Dynamical building simulation: A low order model for thermal bridges losses. *Energy Build.* **2008**, *40*, 2236–2243. [[CrossRef](#)]
16. Tadeu, A.; Simoes, I.; Simoes, N.; Prata, J. Simulation of dynamic liner thermal bridges using a boundary element method model in the frequency domain. *Energy Build.* **2011**, *43*, 3685–3695. [[CrossRef](#)]
17. Berggren, B.; Wall, M. Calculation of thermal bridges in (Nordic) building envelopes—Risk of performance failure due to inconsistent use of methodology. *Energy Build.* **2013**, *65*, 331–339. [[CrossRef](#)]
18. Ascione, F.; Bianco, N.; de Rossi, F.; Turni, G.; Vanoli, G.P. Different methods for the modeling of thermal bridges into energy simulation programs: Comparisons of accuracy for flat heterogeneous roofs in Italian climates. *Appl. Energy* **2012**, *97*, 405–418. [[CrossRef](#)]
19. Capozzoli, A.; Gorrino, A.; Corrado, V. A building thermal bridges sensitivity analysis. *Appl. Energy* **2013**, *107*, 229–243. [[CrossRef](#)]
20. Construction Technical Regulation STR 2.01.02: 2016; *Design and Certification of Energy Performance of Buildings*; Ministry of Environment: Vilnius, Lithuania, 2020.
21. Cerneckiene, J.; Zdankus, T.; Valancius, R.; Fokaides, P.A. Numerical Investigation of the impact of longitudinal thermal bridging on energy efficient buildings under humid continental climate conditions: The Case of Lithuania. In *IOP Conference Series: Earth and Environmental Science*; IOP Publishing: Bristol, UK, 2020; Volume 410, p. 012105.
22. Fokaides, P.A.; Apanaviciene, R.; Černeckiene, J.; Jurelionis, A.; Klumbyte, E.; Kriauciunaite-Neklejonoviene, V.; Pupeikis, D.; Rekus, D.; Sadauskiene, J.; Seduikyte, L.; et al. Research Challenges and Advancements in the field of Sustainable Energy Technologies in the Built Environment. *Sustainability* **2020**, *12*, 8417. [[CrossRef](#)]
23. De Angelis, E.; Serra, E. Light steel-frame walls: Thermal insulation performances and thermal bridges. *Energy Procedia* **2014**, *45*, 362–371. [[CrossRef](#)]
24. Grudzińska, M.; Brzyski, P. The Occurrence of Thermal Bridges in Hemp-lime Construction Junctions. *Period. Polytech. Civ. Eng.* **2019**, *63*, 377–387. [[CrossRef](#)]
25. Udrea, I.; Popa, R.T.; Mladin, E.C.; Georgescu, M.S.; Ochinciuc, C.V. Thermal bridges evaluation for a Passive House building in Romanian Southern climate. In Proceedings of the 2017 8th International Conference on Energy and Environment (CIEM), Bucharest, Romania, 19–20 October 2017; Proceedings Paper: International Conference on Energy and Environment. pp. 456–459.
26. Sadauskiene, J.; Ramanauskas, J.; Seduikyte, L.; Dauksys, M.; Vasylius, A. A simplified methodology for evaluating the impact of point thermal bridges on the high-energy performance of a passive house. *Sustainability* **2015**, *7*, 16687–16702. [[CrossRef](#)]
27. Rruumala. Available online: <https://www.ruumala.com/lt/metaliniai-ankeriai/ploksti-kronsteinai/> (accessed on 1 March 2022).
28. Lithuanian Passive House. Available online: <https://www.pasyvusnamas.lt/langu-montavimas-siltinimo-sluoksnyje/langu-dezes> (accessed on 1 March 2022).
29. Hallik, J.; Kalamees, T. A new method to estimate point thermal transmittance based on combined two-dimensional heat flow calculation. In Proceedings of the 12th Nordic Symposium on Building Physics (nsb 2020), E3SWeb of Conferences, Tallinn, Estonia, 6–9 September 2020; Volume 172, p. 08005. [[CrossRef](#)]

30. Tsukamoto, Y.; Tomikawa, Y.; Sakagami, K.; Okuzono, T.; Maikawa, H.; Komoto, Y. Experimental assessment of sound insulation performance of a double window with porous absorbent materials its cavity perimeter. *Appl. Acoust.* **2020**, *165*, 107317. [[CrossRef](#)]
31. Tang, S.K. A review on natural ventilation-enabling façade noise control devices for congested high-rise cities. *Appl. Sci.* **2017**, *7*, 175. [[CrossRef](#)]
32. Huang, H.; Qiu, X.; Kang, J. Active noise attenuation in ventilation windows. *J. Acoust. Soc. Am.* **2011**, *130*, 176–188. [[CrossRef](#)]
33. Rockwool. Available online: <https://docplayer.me/3412936-Redair-tm-link-monteringsanvisning.html> (accessed on 1 March 2022).
34. ISO. *EN ISO 14683:2017; Thermal Bridges in Building Construction—Linear Thermal Transmittance—Simplified Methods and Default Values*. International Organization for Standardization: Geneva, Switzerland, 2017.
35. Terentjevas, J.; Šadauskaitė, M.; Šadauskienė, J.; Ramanauskas, J.; Buska, A.; Fokaides, P.A. Numerical investigation of buildings point thermal bridges observed on window-thermal insulation interface. *Case Stud. Constr. Mater.* **2021**, *15*, e00768. [[CrossRef](#)]
36. Lawrence Berkeley National Laboratory (LBNL). THERM—Two-Dimensional Building Heat-Transfer Modeling. 2021. Available online: <https://windows.lbl.gov/software/therm> (accessed on 1 March 2022).
37. Blocon, A.B. HEAT3—Heat Transfer in Three Dimensions. 2021. Available online: <https://buildingphysics.com/heat3--3/> (accessed on 1 March 2022).
38. Claesson, J. Dynamic thermal networks: A methodology to account for time-dependent heat conduction. In Proceedings of the 2nd International Conference on Research in Building Physics, Leuven, Belgium, 14–18 September 2003; pp. 407–415.
39. Krawczyk, D.A. Optimization of Energy Consumption while Maintaining Recommended Indoor Air Quality in a Lecture Hall- A case study. In Proceedings of the 16th International Conference on the Sustainable Energy Technologies, Bolonia, Italy, 17–20 July 2017.
40. Nait, N.; Bourbia, F.; Bauchahm, Y. Effect of thermal insulation on energy efficiency of the building envelope-semi dry climates. In Proceedings of the Advances on Sustainable Cities and Building Development, Sb-Lab 2017, Porto, Portugal, 15–17 November 2017.
41. Misiopceki, C.; Bouquin, M.; Gustavsen, A.; Jelle, B.P. Thermal Modeling and Investigation of the Most Energy-Efficient Window Position. *Energy Build.* **2018**, *158*, 1079–1086. [[CrossRef](#)]
42. Ascione, F.; Bianco, N.; De Masi, R.F.; Mauro, G.M.; Musto, M.; Vanoli, G.P. Experimental validation of a numerical code by thin film heat flux sensors for the resolution of thermal bridges in dynamic conditions. *Appl. Energy* **2014**, *124*, 213–222. [[CrossRef](#)]
43. Šadauskiene, J.; Ramanauskas, J.; Vasylius, A. Impact of point thermal bridges on thermal properties of building envelopes. *Therm. Sci.* **2020**, *24*, 2181–2188. [[CrossRef](#)]
44. Ilomets, S.; Kuusk, K.; Paap, L.; Arumagi, E.; Kalamees, T. Impact of linear thermal bridges on thermal transmittance of renovated apartment buildings. *J. Civ. Eng. Manag.* **2016**, *23*, 96–104. [[CrossRef](#)]